Structural Engineering and Mechanics, *Vol. 52, No. 3 (2014) 541-558*
DOI: http://dx.doi.org/10.12989/sem.2014.52.3.541

Seismic rehabilitation of RC frame using epoxy injection technique tested on shaking table

Jiangtao Yu*, Yuanmiao Zhang and Zhoudao Lu

Research Institute of Structural Engineering and Disaster Reduction, Tongji University, Shanghai, China

(Received October 11, 2013, Revised May 6, 2014, Accepted June 23, 2014)

Abstract. A 1/4-scale two-bay eight-storey reinforced concrete frame was tested on shaking table. Initial shaking table tests were carried out through a set of real seismic excitations to investigate the seismic behavior of the RC frame. Subsequently, the damaged frame was repaired using epoxy injection technique, and then subjected to the tests with the same records. The purpose of this study was to investigate experimentally the dynamic characteristics, cracking pattern and lateral inter-story stiffness of RC frames using epoxy injection technique. The test results indicate that epoxy-injection technique appears to be a satisfactory method for repairing earthquake-damaged structure.

Keywords: reinforced concrete frame; shaking table test; epoxy injection technique; dynamic characteristic; wedge splitting test

1. Introduction

In recent major earthquakes (China 2008, Italy 2009, Haiti and Chile 2010), many reinforced concrete (RC) frame structures were damaged severely for two reasons: 1) a part of reinforced concrete structures designed according to conventional codes had deficient lateral load resistance and insufficient energy dissipation. These RC structures may have a non-ductile reinforcement detailing in the beam-column joint area in terms of inadequate transverse reinforcements or weak-column/ strong-beam design according to old codes (without seismic details); 2) the structures designed and constructed according to current codes (with seismic details) were subjected to high-intensity earthquake whose intensity was higher than seismic precautionary intensity. Post-earthquake investigations showed that most of the damaged RC frames were considered repairable. From an economic standpoint, it is surly more desirable to repair such damage than to demolish an old one and construct a new structure. Additionally, the new "Seismic ground motion parameter zonation map of China (GB 18306-2001, 2001) has been published to make an adjustment on the seismic intensity factors. In certain zones, the new factors in this map are higher than in the previous code for the same zones. These new data reflect possible deficient resistance of many structures in this area, under the effects of an expected strong earthquake. This also raises the need for upgrading the seismic performance of this type of structures.

Alternative retrofit and strengthening solutions for reinforced concrete structure have been

*Corresponding author, Ph.D., E-mail: yujiangtao@tongji.edu.cn

http://www.techno-press.org/?journal=sem&subpage=8 ISSN: 1225-4568 (Print), 1598-6217 (Online)

studied in the past and adopted in practical applications. Generally, for cracked or crushed RC structure, a widely adopted method is filling the damaged place with high strength materials and then strengthening it by high-performance composite material, such as FRP material (Balsamo 2005, Niroomandi 2010, Garcia 2010, Zhu 2011, Altin 2008, Erdem 2006, El-Sokkary 2009, Zou 2007, Karayannis 2008). From the retrofitting effect point of view, this method is effective in both repairing and strengthening. But in a scientific study, it is hard to distinguish the respective contributions of crack filling and composite reinforcement. It is a fair question to define the effect of crack repairing when retrofitting damaged RC structures.

In the last several decades, epoxy-injection technique was extensively applied to repair the cracking of RC structures in low or moderate damage level. But so far, only limited experimental research works have been published about the effectiveness of this technique on seismically damaged RC structure. Adin *et al*. (1993) carried out a quasi-static test to evaluate the cyclic behavior of reinforced concrete beam-column joints repaired by epoxy. The comparison between the response of the specimens before and after repair clearly indicated considerable increase in stiffness, general yield resistance, envelope stiffness, and ultimate resistance with energy-dissipation capacity. Karayannis *et al*. (1998) also tested the effectiveness of 17 exterior RC beam-column connections repaired using epoxy resin infused under pressure into the crack system of damaged joint body. The repaired specimens compared with the virgin ones exhibited equal or higher load-carrying capacities, loading stiffness of the same level and increased hysteretic energy absorption capability. The repaired specimens also sustained more full loading cycles without significant loss of strength or stiffness. Issa *et al*. (2007) adopted epoxy compounds to restore the integrity of cracked specimens by gravity filling of the crack. The test results indicated that, compared with control specimens, the compressive strength of cracked concrete test cubes and repaired cubes respectively decline 40.93% and 8.23%. French *et al*. (1990) investigated the effectiveness of epoxy techniques to repair moderate earthquake damage. The specimens after the initial damage were repaired with one of the two epoxy repair techniques: pressure injection or vacuum impregnation and re-tested. Their experiment results indicated the epoxy repair techniques worked well in restoring the strength, stiffness, energy-dissipation capacity, and bond of the specimens.

The above-mentioned literatures fully validated the effectiveness of epoxy-injection technique on repairing damaged RC components. Compared with the damage occurred in RC components, degradation of a whole RC frame is surly far more comprehensive. All the local damages in component level, normally including concrete cracking, concrete crush, rebar buckling and rebar fracture, will all be reflected in the global response of whole structure. On the other hand, in the process of repairing, with the recovering of damaged RC components, the whole structure will surely regain its strength gradually. However, limited studies had been concentrated on the retrofitting of a whole structure, say RC frame, repaired by epoxy injection.

The main objective of this paper is to validate the effectiveness of epoxy repair for RC frame. For this purpose, a 1/4-scale, two-bay, eight-story, reinforced concrete frame was constructed for experimental study. The following contents are involved in the tests:

a) Wedge splitting tests were conducted on six specimens made of the concrete from the RC frame. After repairing by epoxy-injection, the specimens were retested. The effectiveness of repair was investigated by the comparison of fracture energy and double-K fracture parameters from the original and repaired specimens; b) The global behavior and damage pattern were observed; c) The variations of dynamic characteristics (natural frequency, damping ratio) throughout the whole process were investigated and simulated by ABAQUS. d) The calculation results of the lateral

inter-story stiffness of the original structure and the repaired structure were compared.

2. Repairing tests of concrete specimens

To study the feasibility of restoring concrete with epoxy injection, six prisms, namely SW-1~SW-6, were simultaneously cast with the RC frame model. The dimensions of prism are depicted in Fig. 1. A closed-loop servo controlled hydraulic jack with a maximum capacity of 1,000 kN was employed to conduct a so called "wedge splitting test (WST)" (DL/T 5332-2005 2005, Xu 1999). Two clip-on extensometers were installed at the mouth and the tip of the precast notch to measure the crack mouth opening displacement (CMOD) and the crack tip opening displacement (CTOD). To obtain the complete load-deflection curve (P-CMOD), the test rate was fixed at 0.2 mm/min, and it took approximately 30 min to complete a single test of specimen. The initial curves of P-CMOD were obtained by the first splitting, and then the split specimens were repaired with epoxy. RSW-1~ RSW-6 designates the repaired prisms.

The specimens were repaired with two kinds of epoxy resin, namely XH160A/B and XH111 Normal A/B applied by Araldite Company. XH160A/B, with very low viscosity was used for crack

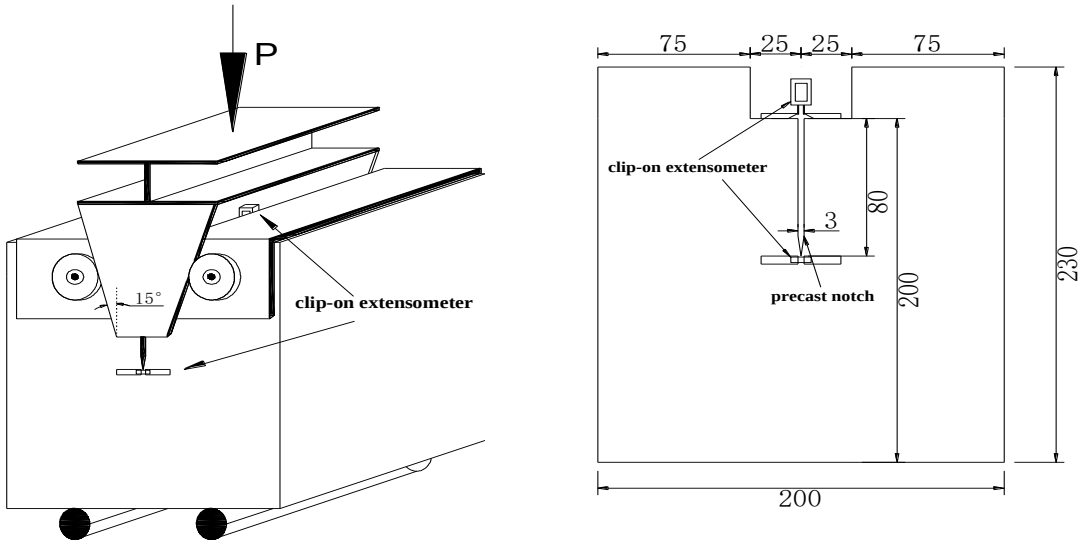

Fig. 1 Configuration of WST: (a) loading arrangement, (b) specimen shape

Table 1 Mechanical property of epoxy (after 7 days at 20℃)

Index	XH160A/B	XH111 Normal A/B
Compressive strength	75N/mm^2	73 N/mm^2
Tensile strength	18N/mm^2	36 N/mm^2
Flexural strength	48N/mm^2	59 N/mm^2
Bond strength to concrete	31N/mm^2	3.62 N/mm^2
Modulus of elasticity	22300N/mm^2 (in compression)	4500N/mm^2 (in tension)

(a) (b)

Fig. 2 Fracture locations of specimens in initial test and re-testing: (a) cracks location of specimen, (b) fractural surface of specimen

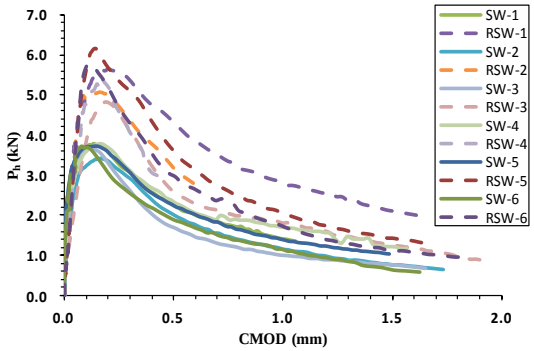

Fig. 3 P-CMOD curves of specimens from initial test and re-testing

penetration to ensure crack filling; XH111 Normal A/B with high viscosity was used for sealing the outer perimeter of crack. The mechanical properties of epoxy resins are presented in Table 1 as reported by the manufacturer.

After curing for 7 days, the repaired prisms were split again. Fig. 2 shows the fracture locations of specimens in initial and re-splitting tests. In the re-testing, cracks of all 6 prisms initiated and propagated in new ways. No repaired crack was opened again. Fig. 3 shows the variation of P-CMOD curves. Comparison of P-CMOD curves shows that the peak loads and embraced area of repaired specimens are both higher than that of initial ones, which indicates the improvement in load bearing capacity and fracture energy of the repaired specimens.

From the P-CMOD curves, the initial crack load (P_{ini}), peak load ($P_{\max}$), initial fracture toughness (K_{1c}^{ini}), unstable fracture toughness (K_{1c}^{un}) (BO 2006) and fracture energy (G_F) (Xu 2003) were calculated and listed in table 2. In the initial WST, the average values of P_{ini}, $P_{\max}$ and G_F are 2.48 kN, 3.68 kN and 128.73 N/m. In the re-splitting test, the corresponding values achieve 3.58 kN, 5.76 kN and 197.86 N/m with increase of 42.14%, 49.70% and 61.66%, respectively. The average value of K_{1c}^{ini} is increased from 0.18 MPa.m1/2 to 0.25 MPa.m1/2, while that of K_{1c}^{un} rise from 0.45 MPa.m$^{1/2}$ to 0.52 MPa.m$^{1/2}$, which show increments of 40.7% and 24.34%, respectively.

On the basis of the WST, it's reasonable to infer the properties of fractured concrete can be restored or even enhanced through epoxy injection technique. This strengthening can be attributed

Table 2 Results from wedge splitting tests

Specimen	P_{ini} (kN)	$P_{\max}$ (kN)	K_{1c}^{ini} (MPa.m$^{1/2}$)	K_{1c}^{un} (MPa.m$^{1/2}$)	G_F (N/m)
SW	2.48	3.68	0.18	0.45	128.73
RSW	3.58	5.76	0.25	0.52	197.86
Growth (%)	42.14	49.7	40.71	24.34	61.66

Table 3 Similarity coefficient of model

Variable	Scaling factor
Length	1/4
Elastic modulus	0.3
Stress	0.3
Poisson ratio	1.0
Density	1.0
Mass	1.56×10^{-2}
Damping	3.42×10^{-2}
Period	0.46
Frequency	2.17
Speed	0.55
Acceleration	1.2
Acceleration of gravity	1.0

to the migration of cracks. It is known that crack always occur at the most vulnerable region of structure, which refers to the least favorable region under loading or the defective region owing to the scattered material or poor construction. In initial WST, cracking revealed the most vulnerable regions in prisms. And then fracture surfaces were repaired by epoxy resin which greatly enhanced the fracture properties of the surfaces. Accordingly it made the second-most vulnerable region be the weakest part in prism. Thus, no repaired crack was opened again and the second-most vulnerable region became the first choice of cracking. Obviously, compared with the initial cracks, new cracks would be surely able to consume more fracture energy and result in higher fracture performance.

3. Shaking table model test of RC frame model

3.1 Model design

A 1/4-scale two-bay eight-story RC frame was constructed for shaking table test. Table 3 lists the similarity coefficient of model. The frame was 3.4 m×3.4 m in plan and had a constant storey height of 0.75 m. The cross sections of column and beam were uniformly 150 mm×150 mm and 125 mm×50 mm, respectively. The specifications of rebar engaged in construction were #10, #12, #14, #16 and #20, of which the diameters were 3.50 mm, 2.77 mm, 2.11 mm, 1.60 mm and 0.90 mm respectively. The thickness of slabs was 30 mm. A general view of the frame along with details of the general geometry, element sections and corresponding reinforcement are shown in Fig. 4 and Fig. 5. Model concrete, with a ratio of 0.76:1:4.58:1.69 was made of recycled aggregate

Table 4 Elastic modulus and strength of concrete

Floor number	Compressive strength (MPa)	Elastic modulus (MPa)
8	5.49	5173
7	4.04	8654
6	5.48	9470
5	3.75	9436
4	12.62	16703
3	9.08	15383
2	9.22	12278
1	9.02	14132

(a) (b)

Fig. 4 Facade view of initial model frame and repaired model frame: a) the initial model frame, b) the repaired model frame

served as course aggregate and fresh sand served as light aggregate. Elastic modulus and strength of the concrete of each storey are listed in Table 4. The total weight of the model was 23560 kg.

3.2 Instrumentation and test program

The shaking table test was conducted in the State Key Laboratory for Disaster Reduction in Civil Engineering at Tongji University. Totally 12 displacement transducers (designated by capital letter *D*) and 28 accelerometers (designated by capital letter *A*) were installed to measure the lateral displacement and acceleration, as shown in Fig. 5. Accelerometers were set on the external-middle joints in both *X* and *Y* directions at each floor, as well as in both *X* (on the corner columns) and Z directions at every two floor, i.e., the ground floor, 2nd floor, 4th floor, 6th floor and 8th floor. Displacement transducers were set at the ground floor and roof floor in both *X* and *Y* directions to measure the absolute displacement. 8 displacement transducers were placed at beam ends at the 2nd floor to measure the angular rotations near joints.

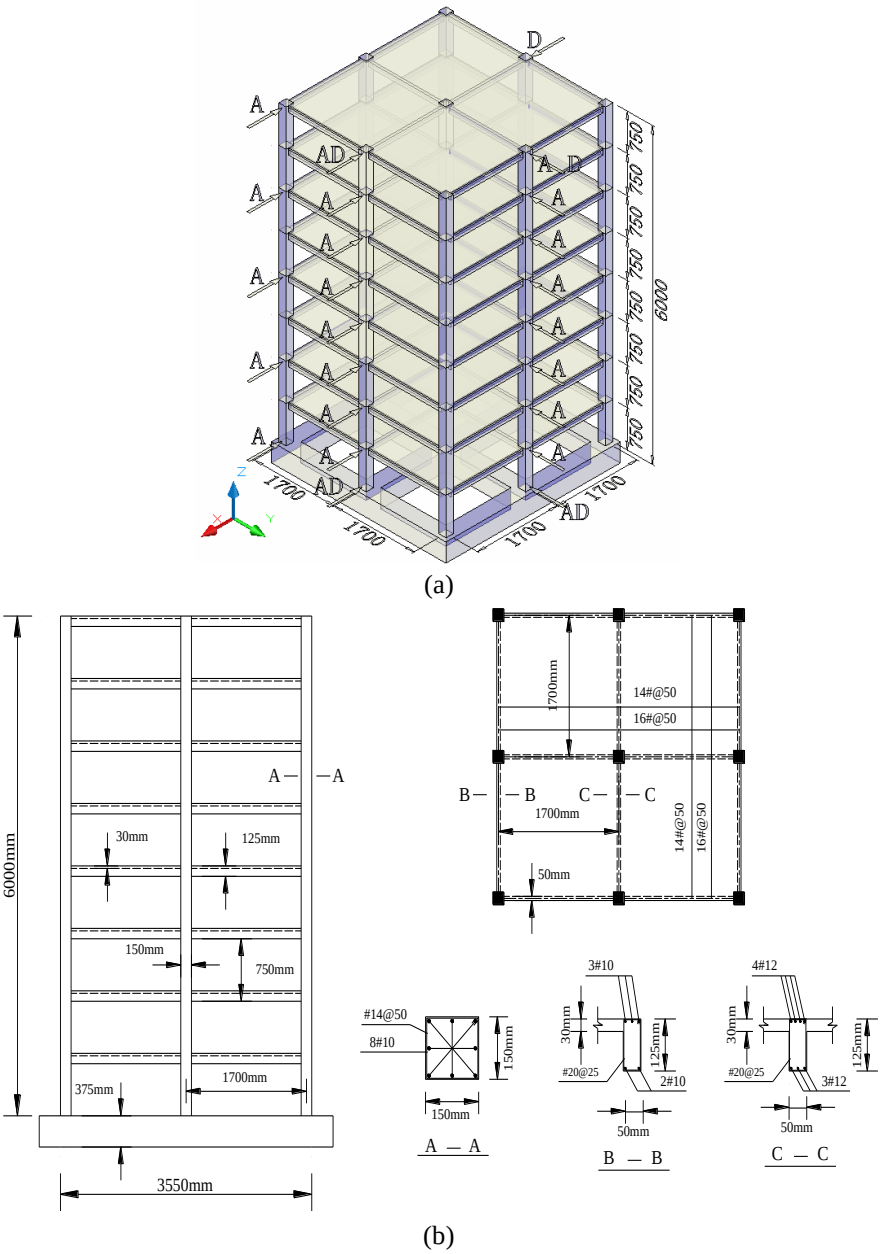

Fig. 5 The layout of displacement & acceleration transducers and framework model: (a) sensors distribution, (b) element sections and corresponding reinforcement

Four kinds of ground motions were inputted to the shaking table, namely El Centro record (E), Kobe record (K), Wenchuan record (W) and MYG013 record (M). These inputs were divided into 4 phases, i.e., frequently occurring (Frequent 8), basic (Basic 8), rarely occurring earthquakes of intensity 8 (Rare 8) and rarely occurring earthquake of intensity 8.5 (Rare 8.5). Wenchuan record, MYG013 record, El Centro record and Kobe record were subsequently inputted in shaking table

during each phase. In the interval of two phases, white noise (WN) tests were undertaken to acquire the model dynamic characteristics including frequency and damping ratio. A summary of the inputs in the test is listed in Table 5.

3.3 Epoxy injection procedure

After the initial test, the width and quantity of cracks was statistically analyzed. All the cracks can be categorized into four levels by width: 1) 0.01 mm< width< 0.10 mm; 2) 0.10 mm≤ width< 0.30 mm; 3) 0.30 mm≤ width< 1.00 mm; 4) width≥ 1.00 mm. Also the cracks or damage can be categorized by location: 1) broad cracks and concrete crushing occurred at the interfaces of beam and column; 2) diagonal and vertical (flexural and shear mixed crack) cracks appeared nearly the ends of beam; 3) small cracks propagated from the bottom of beams at mid-span; 4) Except several fine cracks on the ground floor columns, horizontal cracks are concentrated at floor levels above 5th. Concrete crushing occurred near the top floor. 5) Cracks occurred in the negative moment regions of slabs. The quantity of cracks categorized by width and location were listed in Table 6. Compared with that at upper floors, damages in the lower floors were relatively slight.

Table 5 Loading cases of earthquake motion excitation

Test cases	Phase	Case name	1/4 Model (*Sa*=1.2)			Test cases	Phase	Case name	1/4 Model (*Sa*=1.2)		
			Direction *X*/g	Direction *Y*/g	Direction *Z*/g				Direction *X*/g	Direction *Y*/g	Direction *Z*/g
1	WN1	1WN	0.05	0.05	0.05	17		E2	0.24	0.204	0.156
2		W1	0.084	0.072	—	18		K2	0.24	0.204	0.156
3		M1	0.084	0.072	—	19	WN 3	3WN	0.05	0.05	0.05
4		E1	0.084	0.072	—	20		W3	0.48	0.408	—
5	Frequent 8	K1	0.084	0.072	—	21		M3	0.48	0.408	—
6		W1	0.084	0.072	0.054	22		E3	0.48	0.408	—
7		M1	0.084	0.072	0.054	23	Rare 8	K3	0.48	0.408	—
8		E1	0.084	0.072	0.054	24		W3	0.48	0.408	0.312
9		K1	0.084	0.072	0.054	25		M3	0.48	0.408	0.312
10	WN 2	2WN	0.05	0.05	0.05	26		E3	0.48	0.408	0.312
11		W2	0.24	0.204	—	27		K3	0.48	0.408	0.312
12		M2	0.24	0.204	—	28	WN 4	4WN	0.05	0.05	0.05
13	Basic 8	E2	0.24	0.204	—	29	Rare 8.5	W4	0.612	0.5208	0.3984
14		K2	0.24	0.204	—	30		E4	0.612	0.5208	0.3984
15		W2	0.24	0.204	0.156	31	WN5	5WN	0.05	0.05	0.05
16		M2	0.24	0.204	0.156						

Table 6 Quantity of cracks categorized by width and location

Crack location	Width (mm)			
	0.01~ 0.10	0.10~ 0.30	0.30~ 1.00	1.00~
Mid-span of beam	54	42	2	-
Beam end	45	60	18	12
Interface of joint	-	-	-	131
Column	22	16	4	2

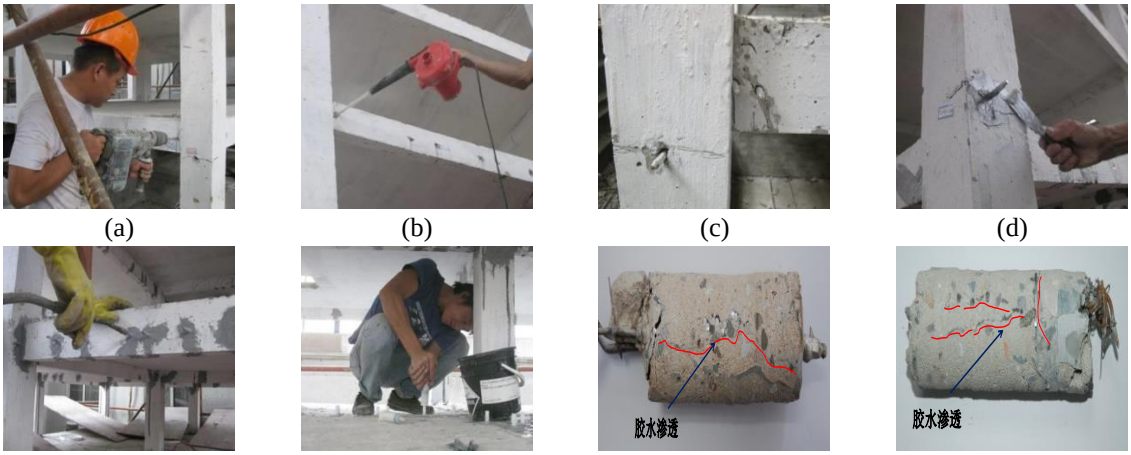

Fig. 6 Process of epoxy-injection technique and concrete samples: (a) hole drilling, (b) hole cleaning, (c) pipe installation, (d) crack surface sealing, (e) pressure injecting, (f) slab crack injecting, (g)~(h) core drilled from the repaired concrete

According to the guidelines of Chinese Code (GB50367-2006 2006), a crack whose width is smaller than 0.2 mm is recommended to be sealed from the outside rather than injection. In actual practice of China, crack injection is generally implemented with syringe pistons forced by elongated rubber bands, which can only provide low pressure when injecting. To guarantee the repairing effect, we decided to repair all the visual cracks with high pressure. A special injection machine was adopted to ensure quality. Fig. 6 presents the main procedures of injection, a) drill small holes perpendicular into the cracking concrete; b) clean dusts and particles from holes with a blower; c) plant steel pipes into drilled holes as inlets of epoxy; d) seal the surface of crack with XH111 Normal A/B, except for steel pipe inlet and outlet for air to escape from inner voids; e) pump epoxy through steel pipe under a specified pressure of 2.4 N/mm^2. This value was designed to make sure a sound filling and at the same time avoid a undesired concrete fracture induced by overpressure. Fig. 6(g)~(h) shows the cores (diameter=60 mm) drilled from repaired concrete. Red lines in Fig. 6(g)~(h) highlighting the filling tracks of epoxy exhibit the desirable effect of such injection technique. Due to the limited thickness of slab (only 40 mm), the conventional method, syringe piston attached with elongated rubber bands is chosen for injection, as shown in Fig. 6(f).

To determine the variation of dynamic characteristics of frame in repairing, epoxy injection was carried out in a specified order. The cracks on beams, column and core joints were repaired from the ground floor to the top roof level. After that, the slab cracks were repaired. To reveal the variation of progressive restoration, artificial impact (AI) test and ambient vibration (AV) test were performed to determine the frequencies and damping of frame. Artificial impact was performed by applying an initial lateral displacement of approximately 2 mm at the top of frame, and then releasing to make a free vibration. Respectively, 19 times of AI and AV tests had been carried out in repairing process. From the test data, natural frequencies and damping ratios were achieved by using the Fourier transform and logarithmic decrement method. The results of measured natural frequencies and damping ratio are presented in Table 8 and Fig. 8~10.

After 28 days curing, then the repaired frame was subjected to the tests with the same input accelerograms selected for the initial.

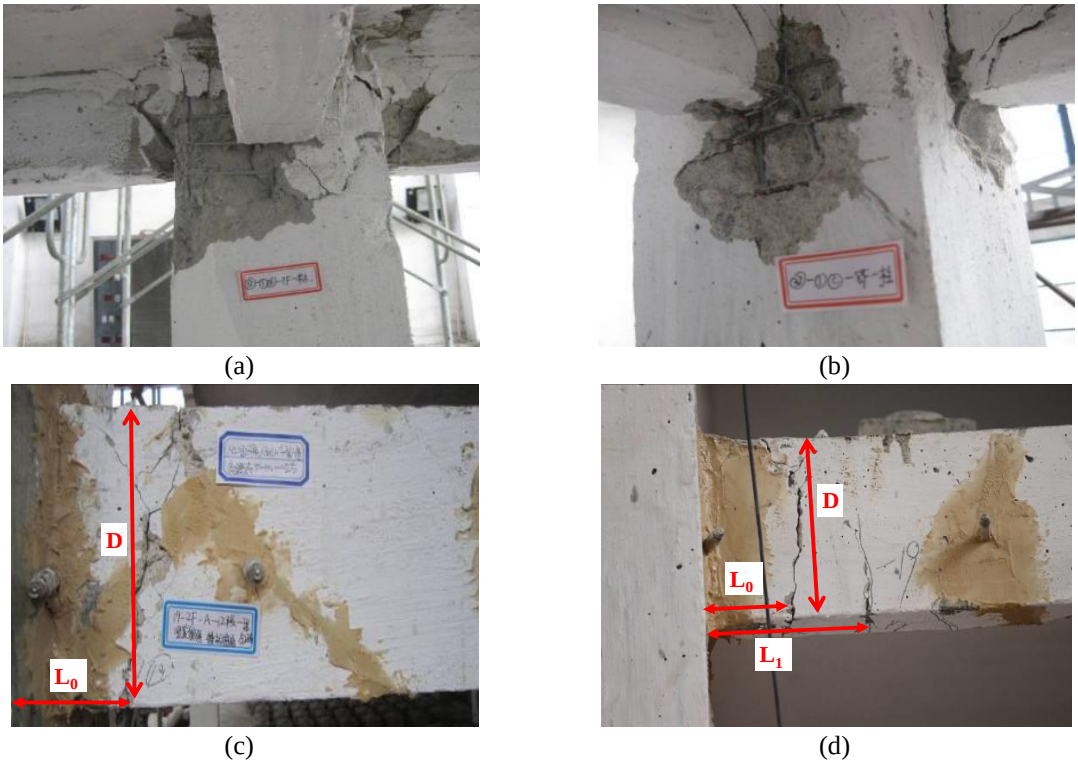

Fig. 7 Comparison of the failure of models in the initial test and re-testing: (a)~(b) Joints damage of the model in initial test, (c)~(d) Joints damage of the model in re-testing (D denotes the height of beam; L_0 and L_1 denote the distance between the new cracks and the column respectively)

4. Test results and discussion

4.1 Failure of the model

Repaired model exhibited the following difference from the original one in failure pattern: 1) all cracks occurred in new regions (without exception)，No repaired crack was opened again in re-testing; 2) failure mode was changed from joint failure to beam end failure and the distance between new crack and juncture of beam and column was at the range of 0.5 to 1 times of beam height, shown in Fig. 7; 3) compared with that in the initial test, the beams of repaired frame damaged more severely in lower floors, but possessed much less amount of cracks at upper floors. The damage level of columns in repaired frame was similar to the initial in lower floors. In upper stories, few cracks were found on the surface of column.

Statistical evaluations about the visual damage of beams were carried out in accordance with four grades. ① Severe damage. Crack penetrated the whole beam section; concrete at end of beam is crushed and fall out, revealing longitudinal steel rebar. ② Moderate damage. Vertical or inclined crack occur; concrete is crushed but not falling out. ③ slight damage. Only a few of fine cracks occur. No crush occurred; ④ No visual damage. Table 7 presents the summary of damage on beam ends in the initial test and re-test. The proportions of severe damage and moderate

Table 7 Summary of the damage on beam ends in the initial test and re-testing

Damage in the initial test							Damage in the re-testing						
Floor	Damage level				Proportion (%)		Floor	Damage level				Proportion (%)	
	①	②	③	④	①	②		①	②	③	④	①	②
1	0	8	16	0	0.00%	33.33%	1	6	15	3	0	25.00%	62.50%
2	0	12	12	0	0.00%	50.00%	2	11	8	2	3	45.80%	33.30%
3	7	4	13	0	29.17%	16.67%	3	13	7	1	3	54.20%	29.20%
4	6	9	9	0	25.00%	37.50%	4	11	7	3	3	45.80%	29.20%
5	8	10	6	0	33.33%	41.67%	5	5	9	7	3	20.80%	37.50%
6	11	11	2	0	45.83%	45.83%	6	2	7	11	4	8.30%	29.20%
7	23	1	0	0	95.83%	4.17%	7	0	15	1	8	0.00%	62.50%
8	14	9	1	0	58.33%	37.50%	8	0	1	1	22	0.00%	4.20%

Table 8 Natural frequency, mode and damping ratio of framework model

Frequency detect case	Test condition	Frequency in *X*-direction (Hz)		Frequency in *Y*-direction (Hz)		Damping ratio (%)	
		AV/WN	FE model	AV/WN	FE model	*X*-direction	*Y*-direction
1	AV (intact frame)	1.87	1.85	1.83	1.85	0.33	0.45
2	WN1 (initial test)	1.70	1.85	1.70	1.85	7.50	4.53
3	WN2 (initial test)	1.49	1.51	1.49	1.52	4.52	6.24
4	WN3 (initial test)	1.06	1.09	0.96	1.05	13.62	12.79
5	WN4 (initial test)	0.85	0.90	0.64	0.78	14.74	12.03
6	WN5 (initial test)	0.74	0.68	0.64	0.68	22.29	20.85
7	AV (before repair)	1.05	0.68	0.74	0.68	5.59	9.11
8	AV(first story repaired)	1.12	0.76	0.84	0.75	-	7.01
9	AV(Second story repaired)	1.20	0.84	0.99	0.80	6.97	5.86
10	AV(Third story repaired)	1.27	1.01	1.12	0.93	4.72	7.92
11	AV(Forth story repaired)	1.40	1.14	1.40	1.06	4.48	4.47
12	AV(Fifth story repaired)	1.55	1.37	1.58	1.29	4.17	2.43
13	AV(Sixth story repaired)	1.72	1.59	1.76	1.54	1.58	1.64
14	AV(Seventh story repaired)	1.76	1.78	1.76	1.76	1.10	1.16
15	AV(Eighth story repaired)	1.86	1.85	1.86	1.85	2.70	1.58
16	WN1 (re-test)	1.59	1.85	1.59	1.85	5.68	8.74
17	WN2 (re-test)	1.49	1.47	1.49	1.50	5.59	5.73
18	WN3 (re-test)	1.17	1.17	1.27	1.21	6.58	7.57
19	WN4 (re-test)	0.85	0.90	0.96	0.81	10.96	13.71
20	WN5 (re-test)	0.85	0.72	0.85	0.78	10.99	15.00
21	AV (after re-test)	1.17	0.72	1.17	0.78	1.93	2.88

damage were also listed in Table 7. The data in Table 7 indicate the repaired frame damaged seriously in lower floors and slightly in upper floors, which was apparently different with respect to the initial one.

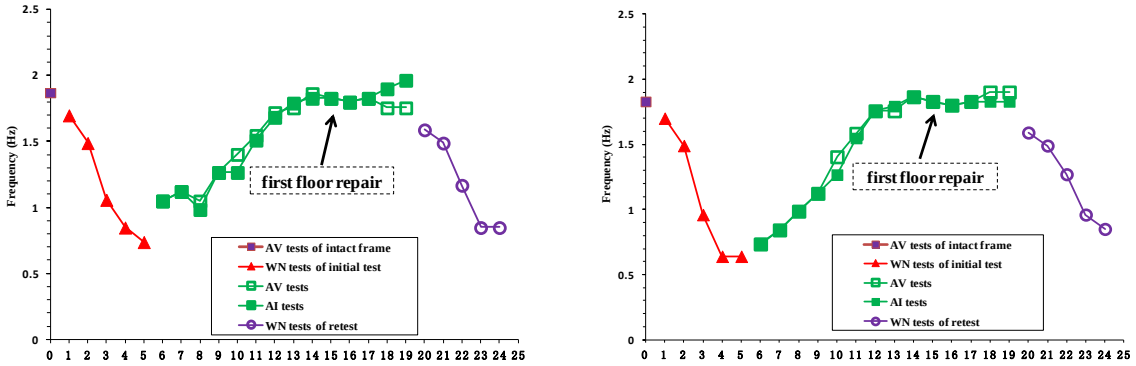

Fig. 8 Variation of the natural frequency: (a) *X*-direction, (b) *Y*-direction

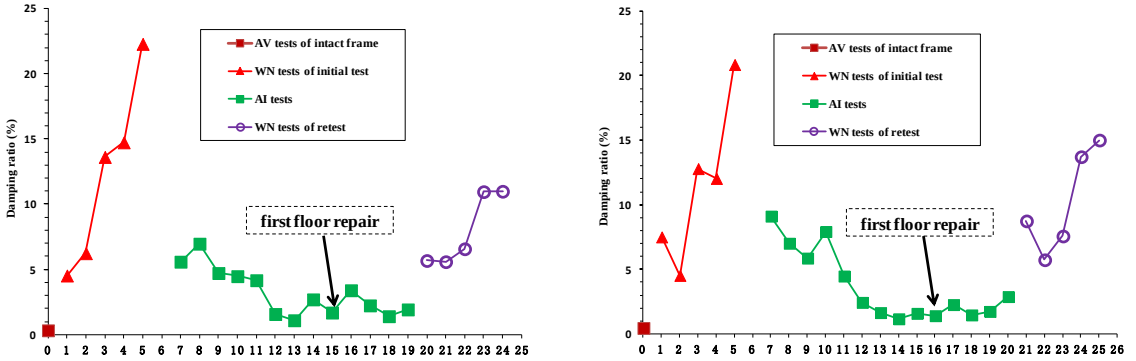

Fig. 9 Variation of damping ratio: (a) X-direction, (b) Y-direction

4.2 Variation of dynamic characteristics

The variations of dynamic characteristics, including natural frequency, damping ratio throughout the whole process by ambient vibration (AV) test, artificial impact (AI) test and white noise (WN) test were studied in this section. The measured natural frequency and damping ratio in initial test, repairing process and re-test are listed in Table 8 and shown in Fig. 8~9. In the initial test and re-testing, dynamic characteristics at different phases were obtained by WN test. In the repairing process, AI and AV tests were employed for frequency and damping ratio. As shown in Fig. 8, the measured results of AI tests and AV tests were fairly close to each other. Thus, only AV test results are listed in Table 8.

It is very evident in Fig. 8 that there are progressive frequency reductions in double shaking table tests and progressive restoration in repairing process. Fig. 9 demonstrates the opposite variation of damping ratio. Frequency increased gradually and damping ratio decreased gradually when cracks were repaired floor by floor; frequency and damping ratio kept almost constant when slabs were repaired. In general, the cracks repairing cause a increase in frequency of the model in *X* direction and *Y* direction respectively up to 77.14% and 151.35%, namely from 1.05 Hz and

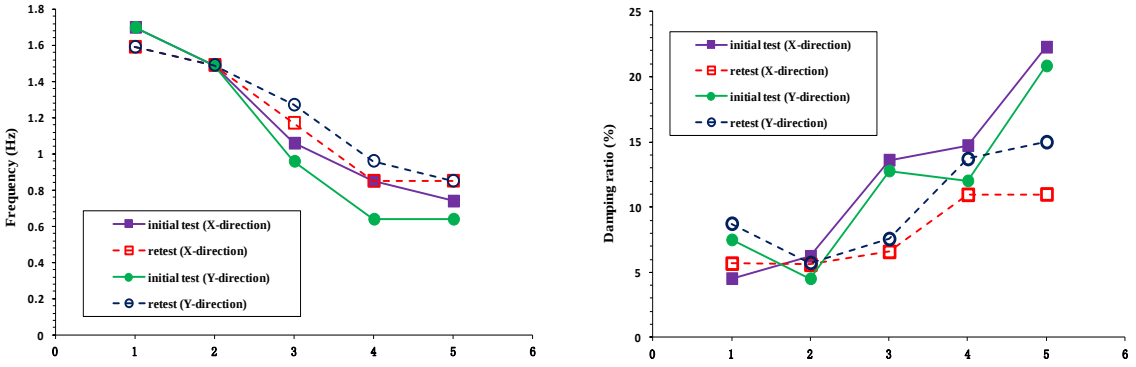

(a) (b)

Fig. 10 Comparison of natural frequency and damping ratio from initial test and re-test: (a) frequency comparison, (b) damping ratio comparison

0.74 Hz to 1.86 Hz and 1.86 Hz, respectively. Besides, repairing made damping ratios in *X* direction and *Y* direction decrease respectively by 65.47% and 68.39%, namely from 5.59% and 9.11% to 1.93% and 2.88%.

As shown in Fig. 10(a), the natural frequency consistently dropped with the increase of the ground peak acceleration (PGA). Through the whole damage process, the natural frequencies of the initial model in *X* direction and *Y* direction reduced by 56.47% and 62.35%, respectively, while that of the repaired model 46.54% and 46.54%. According to the interdependence of stiffness and frequency, the lateral stiffness decreases as the square of frequency reduction. Thus, it is safe to say the frame was severely damaged after initial test and re-test.

What is worth noting is the varying rate of frequency (Fig. 10(a)) and damping ratio (Fig. 10(b)) in the period of initial test and re-testing. Through repairing, frame recovered its natural frequency. But after the excitation of WN1 in re-testing, the frequency dropped to 1.59 Hz, a little lower than 1.70 Hz in initial test. After that, frequency of repaired frame decreases obviously slower. In the test of WN5 in re-testing, the natural frequency 0.85 Hz already exceed those in initial test, which were 0.74Hz and 0.64Hz, respectively. The damping ratio of the model increases with the peak value of acceleration inputs. The final damping ratio of initial frame in X direction and Y direction are respectively 22.29% and 20.85%, while that of the repaired is 10.99% and 15.00% after re-testing. The variation of damping ratio is similar to frequency.

4.3 Variation of the inter-story stiffness of model

The natural frequency variation can reflect lateral stiffness variation of the whole frame. But to figure out the specific effect of epoxy injection, a further analysis is necessary. Based on the measured acceleration and displacement, it was easy to calculate the shear force and inter-story drift ratio of each floor, as well as the secant stiffness that served as the lateral inter-story stiffness. An accurate way to calculate the lateral inter-story stiffness of each floor is using the values of maximal inter-story drift ratio and its corresponding shear force. It is noted that the inter-story drift above includes not only the displacement from lateral force and moment, but also that caused by the rigid body rotation of this and lower floors. Generally, upper floor in a building is affected more from rigid body rotation and consequently illustrates a lower lateral stiffness when compared

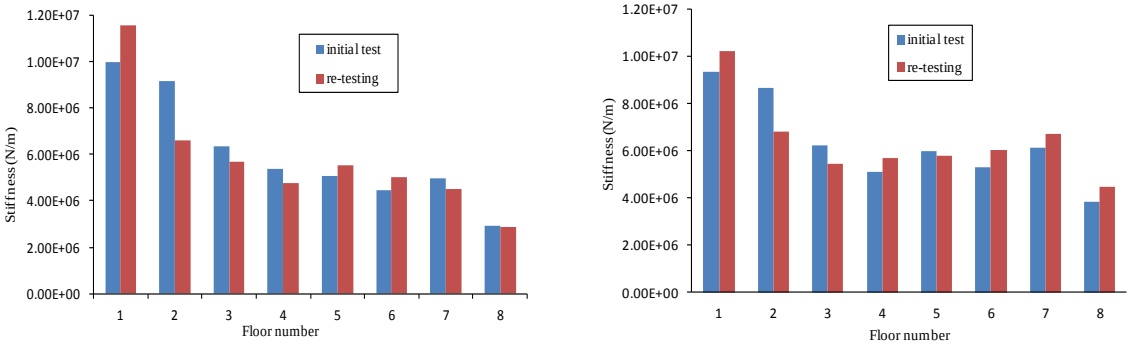

Fig. 11 The inter-story stiffness after loading case 8: (a) *X* direction, (b) *Y* direction

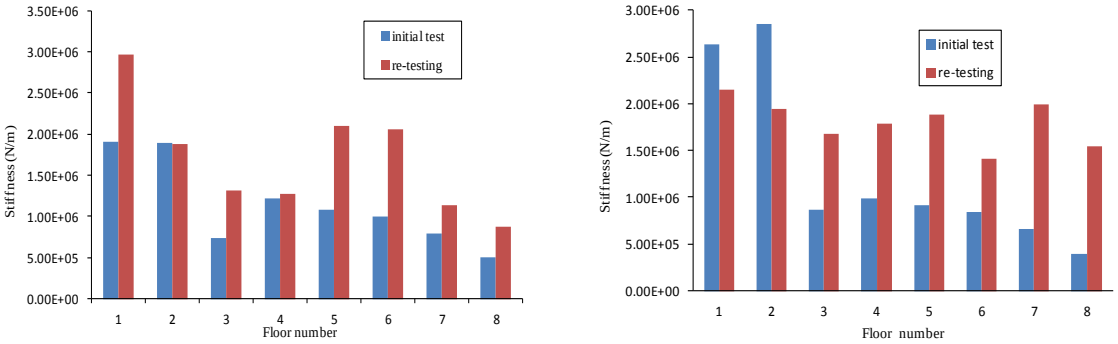

Fig. 12 The inter-story story stiffness after loading case 30: (a) *X* direction, (b) *Y* direction

with the lower floor. In Fig. 11 and Fig. 12, we can see the decline of stiffness by floors.

Due to the limited space, the comparisons of the inter-storey stiffness with respect to only case 8 (Basic 8) and case 30 (Rare 8.5) are listed in Fig. 11 and Fig. 12. Referring to Table 5, loading case 8 represents a comparatively minor excitation, while case 30 represents much stronger motion inputting. From Fig. 11, at minor vibration stage (loading case 8), there was no apparent difference in inter-story stiffness between the initial test and re-testing. But after the last and also highest-amplitude motion (loading case 30) in Fig. 12, the stiffness of repaired model were obviously higher than that of original model at upper floors. In addition, the ground and second floor of repaired model experienced more serious damage comparing the stiffness with the original one. These variations were in fact consistent with the observed results listed Table 7. Frequency detected by WN tests shown the same trend.

Through comparing the stiffness at different floors, the epoxy injection could restore the seismic damage caused in initial test has been proved. To some extent, the repaired frame performed better under high-amplitude motions and became more ductile at the latter stage. It is worth emphasizing that no extra strengthening material was applied to the damaged frame. What was enhanced was the fracture resistance ability of initial cracks, which at last leaded to the migration of crack occurring. The reason has been presented in wedge splitting test.

Fig. 13 ABAQUS model

Through above analysis, the effectiveness of epoxy injection was validated by comparing natural frequency, damping ratio and some sorts of inter-story stiffness.

4.4 Simulation of dynamic characteristics

Through seismic excitation, such as El Centro record, the inter-story stiffness in different phases could be obtained mentioned above as well as the variation of frequency and damping ratio through WN test or AV test. The variation of inter-story stiffness indicated the local damage at each floor, while natural frequency and damping ratio reflected the seismic performance of the global structure. To validate the reliability of the data acquired in this series of tests, we took the derived inter-story stiffness as the basic data to calculate natural frequencies by ABAQUS and made comparisons between the calculated frequencies and measured frequencies. As shown in Fig. 13, a three-dimensional, 8-story, finite element model is established in the general propose program ABAQUS (2011), which totally replicates the RC frame structure. All the beams, columns and slab are simulated using 8-node, linear brick elements C3D8R. The simulation consisted of three major phases including 19 damage states in total. The damage states corresponded to 5 WN tests in initial test (Phase 1), 9 ambient tests in repairing process (Phase 2) and 5 WN tests in re-test (Phase 3).

The first step of simulation was to establish a benchmark FE model at undamaged state, which was used as a reference to quantify damage in the subsequent damage states. In this step, the element property of FE model was defined with data available from tested elastic moduli listed in Table 4. In this way, the frequency of intact frame was obtained by linear perturbation method in ABAQUS, and the initial inter-story stiffness of each floor was predicted.

In order to simulate the damage and rehabilitation process, the elastic modulus of concrete in each floor was reduced or recovered as same as the reduction or increase degree of each floor's inter-story stiffness. In the damage process, as mentioned above, based on the measured acceleration and displacement at each floor level, we derived the inter-story stiffness corresponding to the maximal drift ratio in loading case 8, 17, 26 and 30, which were carried out

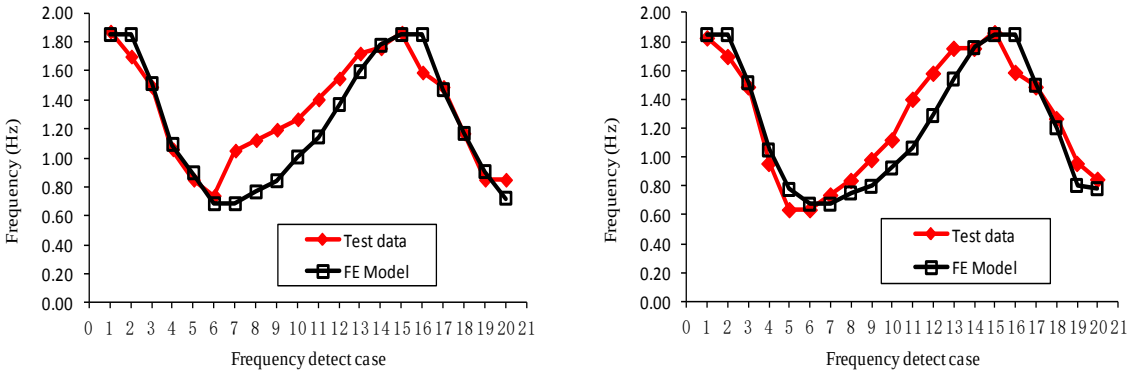

Fig. 14 Comparison of ABAQUS data and test results: (a) X direction, (b) Y direction

right before WN tests. Comparing the inter-story stiffness with the initial undamaged stiffness, stiffness deterioration at each floor was obtained. Using material elastic modulus reduction to reflect stiffness deterioration, we predicted the frequency variation in Phase 1 and Phase 3. In the period of repairing, namely Phase 2, the progressive restoration of inter-story stiffness was simulated by changing the elastic modulus from floor by floor. At the end of repairing, the elastic modulus of each floor was equal to that of benchmark model that meant full-recovery of damage. The progressive restoration of frequency was also listed in Fig. 14.

As shown in Fig. 14, the FE model performed well in simulating the variation of frequency obtained by WN tests, i.e., phase 1 and phase 3. The accurate prediction in frequency verified the reliability of data acquired in the tests, which can infer that the secant stiffness measured from the maximal inter-story drift ratio represents the actual damage state of the RC frame model and can be chosen to serve as lateral inter-story stiffness. However, it should not be ignored that the FE model consistently underestimated the natural frequencies in Phase 2. The gaps between test data and FE prediction can be attributed to the following points:

Firstly, stronger motion makes lower frequency. Numerous literatures have validated structure frequency are close related with the magnitude of excitation (Moaveni 2011, Celebi 1996). In this study, we could also find evidences from test data. As was presented in Table 4, the AV test of the intact frame got natural frequencies 1.87 Hz and 1.83 Hz in *X* and *Y* direction, respectively. In the following WN1 (initial test), they dropped to uniform 1.70 Hz. After the initial test, WN5 (initial test) showed the natural frequencies were 0.74 Hz and 0.64 Hz in *X* and *Y* direction. In the following AV test before repair, the frequencies rose suddenly to 1.05 Hz and 0.74 Hz in *X* and *Y* direction. After repair, AV test obtained the frequencies of 1.86 Hz in both *X* and *Y* direction. In the following WN1 (initial test), frequencies again dropped to 1.59 Hz in double directions. The WN5 (re-test) showed natural frequencies of 0.85 Hz in both directions, while the frequencies detected by AV (after re-test) were uniform 1.17 Hz. It should be noted that no extra excitation had been applied between those frequency tests. The only difference was the vibration amplitude between AV test and WN test. Compared with micro-vibration in AV or AI test, WN motion (GPA is 0.05g) was obviously much stronger. Thus, the natural frequencies measured by WN tests were always lower than those of AV test.

Additionally, the simulation results of frequency depended on the values of the model element's elastic moduli that determined by the lateral inter-story stiffness, which represented the actual

damage state of the RC frame model. Therefore, the frequency of the simulation could still reflect the most serious damage. In actual practice, ambient vibration test is extensively adopted to measure the natural frequency and assess structural damage after earthquake. However, the damage assessment results from AV teats shown that the level of damage assessed may not accurately reflect the actual loss of stiffness. Even if the initial frequency of the intact building is available, assessing structural damage by comparing variation of natural frequencies maybe very likely to underestimate the damage level.

5. Conclusions

In this paper, the seismic performance of a 1/4 scaled model was evaluated with the wedge splitting tests and shaking table tests to study the effectiveness of the rehabilitation technique at repairing earthquake-damaged frame structures. According to comparisons between experimental performance of original and repaired structure, the following conclusions are derived:

1) Fracture properties of cracked concrete can be restored or even heightened through epoxy injection technique, which indicated the possibility of applying epoxy injection technique to repair concrete;

2) The variations of dynamic characteristics, such as natural frequency, damping ratio throughout the whole process by micro-tremor test, impact test and white noise test were investigated. The test result indicated a characteristic decrease of natural frequency and an increase of structural damping in the damage process, while the situation was opposite in the retrofitting process. Compared with the initial test, the decline of natural frequencies and the growth of damping ratios were lower in the retesting;

3) The calculation results of the lateral inter-story stiffness of the original structure and the repaired structure showed that at low-amplitude motions, the repaired structure was slightly less stiff than the original structure and at large deflections associated with severe damage, the stiffness of the repaired structure did not degrade as much as that of the original structure, and cracking in the beam-column joints was less severe in the repaired structure after the test than in the initial structure;

4) To validate the reliability of the data acquired in this series of tests, ABAQUS was used to calculate natural frequencies. The FE model performed well in simulating the variation of frequency obtained by WN tests. The accurate prediction in frequency verified the reliability of data acquired in the tests, which can infer that the secant stiffness measured from the maximal inter-story drift ratio represents the actual damage state of the RC frame model and can be chosen to serve as lateral inter-story stiffness. However the simulation results in the repairing process had lower frequency values than the AV test results. Since the results from AV tests did not accurately reflect the actual stiffness. Even if the initial frequency of the intact building is available, assessing structural damage by comparing variation of natural frequencies from AV tests may be very likely to underestimate the damage level.

It is notable that epoxy injection has little effect on the recovery of reinforcement in concrete. If there is any damage to the reinforcement, like over-yielding, buckling or rupture, corresponding retrofitting method should be engaged.

On the basis of the tests results mentioned above, the epoxy-injection technique appears to be a satisfactory method for repairing earthquake-damaged structure.

References

Adin, M.A., Yankelevsky, D.Z. and Farhey, D.N. (1993), "Cyclic behavior of epoxy-repaired reinforced concrete beam-column joints", *ACI Struct. J.*, **90**(2), 170-179.

Altin, S., Anil, Ö., Kara, M.E. and Kaya, M. (2008), "An experimental study on strengthening of masonry infilled RC frames using diagonal CFRP strips", *Compos. Part B: Eng.*, **39**(4), 680-693.

Balsamo, A., Colombo, A., Manfredi, G., Negro, P. and Prota, A. (2005), "Seismic behavior of a full-scale RC frame repaired using CFRP laminates", *Eng. Struct.*, **27**(5), 769-780.

Bo, D. (2006), "Experimental study using wedge-splitting test on compact tension specimens," Master dissertation, Dalian university of technology, China. (in Chinese)

Celebi, M. (1996), "Comparison of damping in buildings under low-amplitude and strong motions", *J. Wind Eng. Indust. Aerodyn.*, **59**(2), 309-323.

DL/T 5332-2005 (2005), *Norm for fracture test of hydraulic concrete*, China Electric Power Press, Beijing, China. (in Chinese)

El-Sokkary, H. and Galal, K. (2009), "Analytical investigation of the seismic performance of RC frames rehabilitated using different rehabilitation techniques", *Eng. Struct.*, **31**(9), 1955-1966.

Erdem, I., Akyuz, U., Ersoy, U. and Ozcebe, G. (2006), "An experimental study on two different strengthening techniques for RC frames", *Eng. Struct.*, **28**(13), 1843-1851.

French, C. W., Thorp, G. A. and Tsai, W. J. (1990), "Epoxy repair techniques for moderate earthquake damage", *ACI Struct. J.*, **87**(4), 416-424.

Garcia, R., Hajirasouliha, I. and Pilakoutas, K. (2010), "Seismic behaviour of deficient RC frames strengthened with CFRP composites", *Eng. Struct.*, **32**(10), 3075-3085.

GB50367-2006 (2006), *Design code for strengthening concrete structure*, China Architecture &Building Press, Beijing, China. (in Chinese)

GB 18306-2001 (2001), *Seismic ground motion parameter zonation map of China*, China Standard Press, Beijing, China. (in Chinese)

Issa, C. A. and Debs, P. (2007), "Experimental study of epoxy repairing of cracks in concrete", *Construct. Build. Mater.*, **21**(1), 157-163.

Karayannis, C. G., Chalioris, C. E. and Sideris, K. K. (1998), "Effectiveness of RC beam-column connection repair using epoxy resin injections", *J. Earthq. Eng.*, **2**(2), 217-240.

Karayannis, C. G. and Sirkelis, G. M. (2008), "Strengthening and rehabilitation of RC beam–column joints using carbon-FRP jacketing and epoxy resin injection", *Earthq. Eng. Struct. Dyn.*, **37**(5), 769-790.

Moaveni, B., Lombaert, G., Stavridis, A., Conte, J. P. and Shing, P. B. (2011), "Damage identification of a three-story infilled RC frame tested on the UCSD-NEES shake table", *Dyn. Civil Struct.* **4**, 145-154.

Niroomandi, A., Maheri, A., Maheri, M. R. and Mahini, S. S. (2010), "Seismic performance of ordinary RC frames retrofitted at joints by FRP sheets", *Eng. Struct.*, **32**(8), 2326-2336.

Shilang, X., Yanhua, Z., Zhimin, W. and Hongbo, G. (2003), "The experimental study on the fracture energy of concrete using wedge splitting specimens", *J. Hydroelec. Eng.*, **4**, 15-22.

Xu, S. and Reinhardt, H. W. (1999), "Determination of double-K criterion for crack propagation in quasi-brittle fracture, Part III: Compact tension specimens and wedge splitting specimens", *Int. J. Fract.*, **98**(2), 179-193.

Zhu, J. T., Wang, X. L., Xu, Z. D. and Weng, C. H. (2011), "Experimental study on seismic behavior of RC frames strengthened with CFRP sheets", *Compos. Struct.*, **93**(6), 1595-1603.

Zou, X. K., Teng, J. G., De Lorenzis, L. and Xia, S. H. (2007), "Optimal performance-based design of FRP jackets for seismic retrofit of reinforced concrete frames", *Compos. Part B: Eng.*, **38**(5), 584-597.